Refined treatment of single-edge diffraction effects in radiometry

ERIC L. SHIRLEY[1,*]

[1] Sensor Science Division, National Institute of Standards and Technology, 100 Bureau Drive, MS 8441, Gaithersburg, MD 20899-8441
*Corresponding author: eric.shirley@nist.gov

Received XX Month XXXX; revised XX Month, XXXX; accepted XX Month XXXX; posted XX Month XXXX (Doc. ID XXXXX); published XX Month XXXX

This work treats diffraction corrections in radiometry for cases of point and extended sources in cylindrically symmetrical three-element systems. It considers diffraction effects for spectral power and total power in cases of Planck sources. It improves upon an earlier work by the author by giving a simpler rendering of leading terms in asymptotic expansions for diffraction effects and reliable estimates for the remainders. This work also demonstrates a framework for accelerating the treatment of extended sources and simplifying the calculation of diffraction effects over a range of wavelengths. This is especially important in the short-wavelength region, where dense sampling of wavelength values is in principle necessitated by the rapidly oscillatory behavior of diffraction effects as a function of wavelength. We demonstrate the methodology's efficacy in two radiometric applications.

OCIS codes: *(050.1960) Diffraction theory; (120.5630) Radiometry; (000.3860) Mathematical methods in physics; (000.4430) Numerical approximations and analysis.*

http://dx.doi.org/10.1364/AO.99.099999

1. INTRODUCTION AND BACKGROUND

The wave nature of light causes diffraction effects that undermine a geometrical-optics understanding of classical radiometry, wherein the product of source radiance and geometrical throughput determines the power received by a detector. Following Rayleigh [1], Lommel [2] presented a description of Fresnel diffraction and its effect on the irradiance pattern downstream from a circular optical element in the case of a point source. Focke [3] and Wolf [4] integrated that pattern and arrived at expressions for the encircled energy in the central region, which is of greater interest when one wants to know diffraction effects on the total flux. National Measurement Institutes in many countries have endeavored to address and demonstrate the relevance of diffraction to radiometry. See, for example, studies by Sanders and Jones [5], Ooba [6], Blevin [7], Steel *et al.* [8] and Boivin [9]. Several of these researchers considered generalization to extended (Lambertian) sources, a formal treatment of which was presented by the author [10] and studied further by Edwards and McCall [11].

Evaluating and accounting for diffraction effects in radiometry can be referred to as including "diffraction corrections." Practical (unfolded) optical systems usually contain more elements than just a source, aperture (or lens, if it is a powered optic) and detector. However, piecewise accounting for diffraction effects because of certain effective source-aperture-detector (SAD) subsets of one's system can often estimate the salient corrections. Treatments beyond this paradigm include that of partial coherence effects by Mielenz [12], which was adopted by Dionne and coworkers [13], as well as by the author, who considered diffraction of light by multiple optics in series [14-16].

This work revisits the SAD problem for cylindrically symmetrical systems in order to improve and systematize the treatment of the related diffraction effects. To date, numerical treatment of diffraction effects is already well-established. Therefore, in principle the cited references would obviate the need for this study. There remains room for improvement, however, for cases of monochromatic radiation at small wavelength λ and Planck radiation at high temperature T, based on analysis of the asymptotic behavior of diffraction effects in these cases. This is because radiation fields' diffraction patterns can be highly oscillatory, requiring dense sampling of diffraction patterns in cases of extended sources, and dense sampling of wavelength values when diffraction effects are considered as a function of λ.

In Ref. [17], the author analyzed such asymptotic behavior and arrived at formulas for diffraction effects in the case of a point source in terms of a large parameter v for monochromatic radiation and a small parameter A for Planck radiation. These and several other quantities are defined in Section 2. It is the particular goal here to overcome certain shortcomings of Ref. [17]. These include the limited number of terms presented for expansions in $1/v$, the form of expansions in A requiring infinite summations for all terms beyond the first, and the remaining difficulties with the treatment of extended sources and/or of treating a large number of wavelengths in the spectral case. Section 3 rearranges leading-order asymptotic expressions in a more convenient form and completes the said summation for the leading four nonzero terms at the lowest powers of A. Section 4 presents a means by which the "main" diffraction effects can be treated with 10-digit accuracy for a wide scope of systems, outside of which numerical treatments can be easily executed. Section 5 presents a means by which "remaining" diffraction effects can be treated likewise. The "main" diffraction effects consider everything except interference of what would be the source's original light wave, allowing for focusing by powered optics, and modifications to it because of diffraction. The "remaining" diffraction effects account for that interference, on the relevant detector area. The "remaining" effects only matter when a detector is overfilled, because the "main" diffraction effects in the underfilled case are deduced from the integrated flux outside of the detector area and hence entirely in the dark region. Section 6 generalizes the aforementioned benefits to the treatment of extended sources, while Section 7 presents a means by which to streamline the treatment of a large number of short wavelengths in the case of monochromatic radiation. Section 8 presents two radiometric applications, and Section 9 presents closing remarks. Additionally, the Appendix provides technical information relevant to the treatment of Planck radiation.

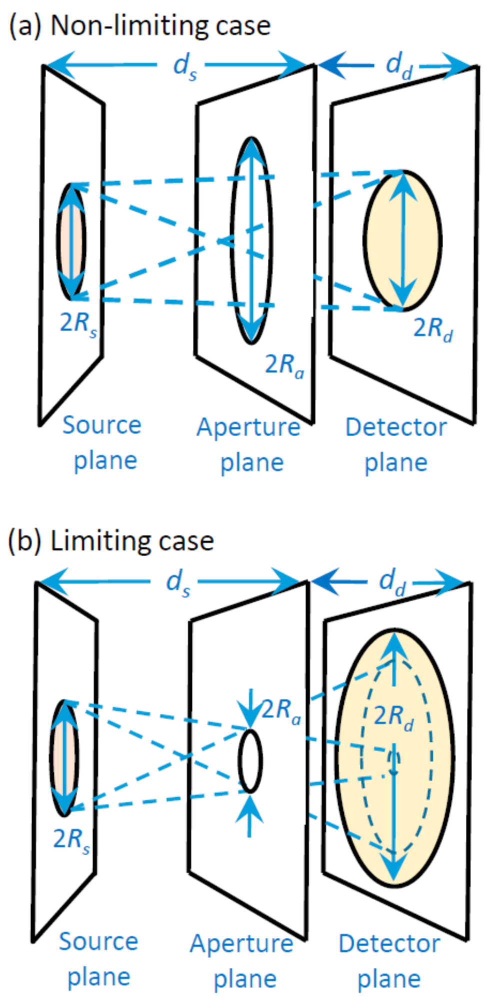

Fig. 1. Source-aperture-detector (SAD) systems considered in this work. The geometries are specified by three radii, R_s, R_a and R_d, two distances d_s and d_d, and (not shown in these cases) the focal length f of the aperture when it is a powered optic.

2. DEFINITION OF THE PROBLEM

Consider the situations illustrated in Fig. 1. In one case, a source illuminates a detector through an aperture, which may be powered, and the detector is overfilled so that the aperture is non-limiting. In the other case, the aperture is limiting, so that the detector is underfilled. In either instance, the source is spatially extended (i.e., it is not an idealized "point source"). Radii of the source, aperture and detector (R_s, R_a and R_d) and the intervening distances (d_s and d_d) are indicated, and we denote the focusing power of the aperture by f, having $f=\pm\infty$ in the unpowered case.

There is a fairly standard notation for dimensionless parameters that can be used in expressions quantifying diffraction effects. These are $u=(2\pi R_a^2/\lambda)(1/d_s+1/d_d-1/f)$, $v_s=(2\pi R_s R_a/\lambda)/d_s$, and $v_d=(2\pi R_d R_a/\lambda)/d_d$. So we have $u\to 0$ in the pinhole-aperture limit and when the source and detector are imaged by the lens onto each other. Two v parameters are necessary in the case of an extended source. By Helmholtz's reciprocity principle v_s and v_d are interchangeable for purposes of calculating diffraction effects. It is helpful to introduce $v_0=\max(v_s,v_d)$ and $\sigma=\min(v_s,v_d)/v_0$, as well as the wavelength-independent length parameter defined according to the pattern, $\alpha=\lambda v$, $\alpha_0=\lambda v_0$, etc. For a point source, with one v parameter $v=(2\pi R_d R_a/\lambda)/d_d$, one can introduce $w=\min(|u|,v)/\max(|u|,v)$. The α and w parameters are equally relevant for monochromatic and Planck radiation.

For a monochromatic point source (the $\sigma\to 0$ limit), Wolf [4] provides a formula for the fraction of flux falling on the aperture that in turn reaches the detector. This is given either by

$$L(u,v)=1-L_B(v,w) \quad \textbf{(1)}$$

for a limiting aperture ($|u|<v$) or by

$$L(u,v)=w^2[1+L_B(v,w)]-L_X(v,w) \quad \textbf{(2)}$$

for a non-limiting aperture ($|u|>v$). Labels $L_B(v,w)$ and $L_X(v,w)$ are a shorthand defined in Ref. [17] for expressions due to Wolf. With $G(\sigma,x)=\{(1-x^2)[(2+\sigma x)^2-\sigma^2]\}^{1/2}/(1+\sigma x)$, spectral power at the detector and spectral radiance of an extended source are related by

$$\Phi_\lambda(\lambda)=CL_\lambda(\lambda)\int_{-1}^{+1}dx\,G(\sigma,x)\,L(u,v_0(1+\sigma x)) \quad \textbf{(3)}$$

with $C=4\pi^3R_a^4R_s^2R_d^2/(d_s^2d_d^2\alpha_0^2)$, which Ref. [17] states incorrectly. This is most easily established for the limiting ($|u|<|v_s-v_d|$) and non-limiting ($|u|>v_s+v_d$) cases, and Edwards and McCall [11] treat other cases.

For Planck radiation, treating diffraction effects on total power reaching the detector involves integration with respect to wavelength over the Planck distribution. If we introduce the dimensionless, temperature-dependent parameter, $A=c_2/(\alpha T)$, where c_2 is the second radiation constant, then considering a Planck radiation source in lieu of a monochromatic source requires the modification of the above analysis according to the replacement

$$L(u,v)\to\int_0^\infty d\lambda\,L(u,v)L_\lambda(\lambda)=\frac{\varepsilon c_1}{\pi\alpha^4}\left[\frac{6\zeta(4)}{A^4}-F_B(A,w)\right] \quad \textbf{(4)}$$

in the limiting case and

$$L(u,v) \to \int_0^\infty d\lambda\, L(u,v) L_\lambda(\lambda) = \frac{\varepsilon c_1}{\pi\alpha^4}\left\{ w^2\left[\frac{6\zeta(4)}{A^4} + F_B(A,w)\right] - F_X(A,w)\right\} \qquad \textbf{(5)}$$

in the non-limiting case. The functions $F_B(A,w)$ and $F_X(A,w)$ are defined implicitly above and are discussed further in Ref. [17]. Here $\zeta(z)$ is the zeta function of Riemann, ε is the source emissivity and c_1 is the first radiation constant. Neglect of diffraction effects amounts to setting $L_B(v,w) = L_X(v,w) = 0$ or $F_B(A,w) = F_X(A,w) = 0$, from which geometrical-optics results for spectral and total power follow.

3. ASYMPTOTIC EXPANSIONS

Reference [17] gives asymptotic expansions for $F_B(A,w)$, $F_X(A,w)$, $L_B(v,w)$ and $L_X(v,w)$. The expansions eventually diverge, but the first several leading terms can be a good approximation in cases of small A or large v.

A. Leading Planck (thermal) terms

At small A, $F_B(A,w)$ is

$$F_B(A,w) = \sum_{s=0}^{\infty} \frac{(-1)^s w^{2s}}{2s+1} I_{2s}(A) \qquad \textbf{(6)}$$

with the asymptotic behavior of each $I_{2s}(A)$ being

$$I_{2s}(A) \sim \sum_{p=-3}^{\infty} (C_{s,p} + L_{s,p} \log_e A) A^p. \qquad \textbf{(7)}$$

Summation over s as prescribed by

$$\left.\begin{aligned} C_p &= \sum_{s=0}^{\infty}\left(\frac{(-1)^s C_{s,p}}{(2s+1)}\right) w^{2s} = \frac{1}{w}\sum_{s=0}^{\infty}\left(\frac{(-1)^s C_{s,p}}{(2s+1)}\right) w^{2s+1} \\ L_p &= \sum_{s=0}^{\infty}\left(\frac{(-1)^s L_{s,p}}{(2s+1)}\right) w^{2s} = \frac{1}{w}\sum_{s=0}^{\infty}\left(\frac{(-1)^s L_{s,p}}{(2s+1)}\right) w^{2s+1} \end{aligned}\right\} \qquad \textbf{(8)}$$

allows for a more convenient form for $F_B(A,w)$:

$$F_B(A,w) \sim \sum_{p=-3}^{\infty} (C_p + L_p \log_e A) A^p. \qquad \textbf{(9)}$$

Including a factor of w in the sum is convenient for analysis below.

The four leading (and typically largest) non-zero terms involve C_{-3}, C_{-1}, L_{-1} and C_0, so that leading relative diffraction effects scale as A. As shown earlier [17], we have $C_{-3} = 4\zeta(3)/[\pi(1-w^2)]$, and we present results of summation for the next three terms and $F_X(A,w)$ below. Our approach is fairly involved, but this treatment simplifies the results of Ref. [17] by allowing for one set of rules to apply when evaluating all terms with odd $p \ge -1$, a possibility not noted earlier. However, closed-form expressions for $p > 0$ are not of as much interest, being somewhat unwieldy, and if such terms are not very small and therefore unimportant, they are probably terms in an asymptotic series that makes poor approximations when A is correspondingly large, so that a more comprehensive (rather than term-by-term) method of evaluating the remainder is desirable.

From Eq. (52-56) of Ref. [17], a $C_{s,p}$ or $L_{s,p}$ coefficient for odd $p \ge -1$ in Eq. (8) is the product of several factors: (1.) respectively, an overall factor $R_{C,p}$ or $R_{L,p}$, which is independent of s:

$$R_{C,p} = +\frac{8\zeta(p+1)}{\pi^{2+p}\Gamma(5+p)2^{6+2p}}, \qquad \textbf{(10)}$$

$$R_{L,p} = -\frac{16\zeta(p+1)}{\pi^{2+p}\Gamma(5+p)2^{6+2p}} = -2R_{C,p}, \qquad \textbf{(11)}$$

(2.) a factor, $(-1)^s(2s+1)$, which cancels an opposite factor in the sum in Eq. (8), (3.) an even polynomial function of $(2s+1)$,

$$\begin{aligned} f_{s,p} &= (2s+1)^2[(2s+1)^2 - (p+3)^2] \\ &\{[(2s+1)^2 - 2^2]\cdots[(2s+1)^2 - (p+1)^2]\}^2, \end{aligned} \qquad \textbf{(12)}$$

with the quantity in curly brackets having only one factor for $p = 1$ and being unity for $p = -1$, and, (4.) only in the case of $C_{s,p}$, a factor, $c_{s,p}$, found in square brackets in Eq. (52) and Eq. (56) of Ref. [17], which is a constant independent of s minus four digamma functions of s plus half-integers.

The digamma function is given by $\psi(z) = d\log_e \Gamma(z)/dz$. Those in $c_{s,p}$ that depend on s can be related to $\psi(s+3/2)$ by successive application of the recurrence relation, $\psi(z+1) = \psi(z) + 1/z$. For integer m, one has

$$\begin{aligned} \psi(s+m+3/2) = \psi(1/2) + [\psi(s+3/2) - \psi(1/2)] + \\ [\psi(s+m+3/2) - \psi(s+3/2)]. \end{aligned} \qquad \textbf{(13)}$$

The second term is

$$\psi(s+3/2) - \psi(1/2) = \sum_{t=0}^{s} \frac{2}{2t+1}. \qquad \textbf{(14)}$$

The third term is zero for $m = 0$, but for $m > 0$ the third term is

$$\psi(s+m+3/2) - \psi(s+3/2) = \sum_{k=1}^{m} \frac{2}{(2s+1)+2k}. \qquad \textbf{(15)}$$

For $m < 0$, it is convenient to set $\mu = -1 - m$, implying $m = -1 - \mu$, to obtain

$$\psi(s+m+3/2) - \psi(s+3/2) = -\sum_{k=0}^{\mu} \frac{2}{(2s+1)-2k}. \qquad \textbf{(16)}$$

The arguments of the four digamma functions always have values so that $c_{s,p}$ has the form (with $p = 1 + 2\tau$)

$$\begin{aligned} c_{s,p} &= r_\tau + \frac{4}{2s+1} - \sum_{t=0}^{s}\frac{8}{2t+1} + \\ &\sum_{k=1}^{(p+3)/2} \frac{16k}{(2s+1)^2 - 4k^2} - \frac{4(p+3)}{(2s+1)^2 - (p+3)^2}. \end{aligned} \qquad \textbf{(17)}$$

This implies

$$f_{s,p} c_{s,p} = r_\tau f_{s,p} + 4 f_{s,p}\left(\frac{1}{2s+1} - 2\sum_{t=0}^{s}\frac{1}{2t+1}\right) + g_{s,p}, \qquad \textbf{(18)}$$

where $g_{s,p}$ is also an even polynomial function of $2s+1$, because the denominators appearing in $c_{s,p}$ that involve $(2s+1)^2$ are all factors of $f_{s,p}$. The leading term is

$$r_\tau = \psi\left(-\frac{5}{2}-\tau\right)+\psi\left(-\frac{1}{2}-\tau\right)+\psi(3+\tau)+\psi(1+\tau)+ 4\gamma+10\log_e 2+2\left(\frac{\zeta'(-1-2\tau)}{\zeta(-1-2\tau)}\right). \quad \textbf{(19)}$$

For $p=\tau=-1$, this uses $\lim_{\tau\to-1} r_\tau = 2\gamma+6\log_e 2+11/3$.

To evaluate

$$L_p = w^{-1}R_{L,p}\sum_{s=0}^{\infty} f_{s,p}\ w^{2s+1} \quad \textbf{(20)}$$

and

$$C_p = w^{-1}R_{C,p}\sum_{s=0}^{\infty} f_{s,p}c_{s,p}w^{2s+1}, \quad \textbf{(21)}$$

one can use the relation

$$(2s+1)w^{2s+1} = \left(w\frac{d}{dw}\right)w^{2s+1} \quad \textbf{(22)}$$

to replace powers of $(2s+1)$ in $f_{s,p}$ and $g_{s,p}$ with action of the operator indicated, in order to relocate the polynomials outside of the sum, making C_p and L_p $1/w$ times combinations of results of even numbers of actions of the operator on

$$S_- = \sum_{s=0}^{\infty} w^{2s+1} = \frac{w}{1-w^2} = \frac{1}{2}\left(\frac{1}{1-w}-\frac{1}{1+w}\right), \quad \textbf{(23)}$$

$$S_L = \sum_{s=0}^{\infty}\frac{w^{2s+1}}{2s+1} = \frac{1}{2}\log_e\left(\frac{1+w}{1-w}\right) \quad \textbf{(24)}$$

and

$$\sum_{s=0}^{\infty}\sum_{t=0}^{s}\frac{w^{2s+1}}{2t+1} = \sum_{t=0}^{\infty}\frac{w^{2t+1}}{2t+1}\sum_{t'=0}^{\infty} w^{2t'} = \left[\frac{1}{2}\log_e\left(\frac{1+w}{1-w}\right)\right]\left(\frac{1}{1-w^2}\right) = S_L S_+, \quad \textbf{(25)}$$

with

$$S_+ = \sum_{s=0}^{\infty} w^{2s} = \frac{1}{1-w^2} = \frac{1}{2}\left(\frac{1}{1-w}+\frac{1}{1+w}\right). \quad \textbf{(26)}$$

Action of the operator on $1/(1-w)$ yields

$$\left(w\frac{d}{dw}\right)^n \frac{1}{1-w} = \frac{W_n(w)}{(1-w)^{n+1}} \quad \textbf{(27)}$$

with $W_0(w)=1$ and, for $n>0$,

$$W_n(w) = w\sum_{k=0}^{n-1}\left\langle {n \atop k}\right\rangle w^k, \quad \textbf{(28)}$$

where angle brackets denote Eulerian numbers. Thus, for $n>0$ the polynomial $W_n(w)$ is w times a palindromic polynomial of w of order $n-1$. It follows that we have

$$\begin{aligned}\left(w\frac{d}{dw}\right)^n S_\pm(w) &= \frac{1}{2}\left(w\frac{d}{dw}\right)^n\left(\frac{1}{1-w}\pm\frac{1}{1+w}\right)\\ &= \frac{1}{2}\left(\frac{W_n(w)}{(1-w)^{n+1}}\pm\frac{W_n(-w)}{(1+w)^{n+1}}\right)\\ &= \frac{1}{2}\left(\frac{(1+w)^{n+1}W_n(w)\pm(1-w)^{n+1}W_n(-w)}{(1-w^2)^{n+1}}\right)\\ &= \frac{\Omega_n^\pm(w)}{(1-w^2)^{n+1}}.\end{aligned} \quad \textbf{(29)}$$

We have $\Omega_0^+(w)=1$ and $\Omega_0^-(w)=w$. For $n>0$, $\Omega_n^-(w)$ is w times a palindromic polynomial of w^2 of order n, and $\Omega_n^+(w)$ is w^2 times a palindromic polynomial of w^2 of order $n-1$, so that $\Omega_n^+(w)$ for even n is also $w^2(1+w^2)$ times a palindromic polynomial of w^2 of order $n-2$. In fact, we have $\Omega_n^+(w)=2^n W_n(w^2)$.

Having $w(dS_L/dw)=S_-$, the effect of multiple actions of the operator on S_L also follows from above. We also have

$$\left(w\frac{d}{dw}\right)xy = x\left(w\frac{d}{dw}\right)y + y\left(w\frac{d}{dw}\right)x, \quad \textbf{(30)}$$

and applying a binomial-theorem generalization of this rule also lets one evaluate the result of multiple actions on $S_L S_+$. This product and S_L always appear in the combination, $S_L - 2S_L S_+$, for which we have

$$\begin{aligned}D_{2n} &= \left(w\frac{d}{dw}\right)^{2n}(S_L-2S_LS_+)\\ &= \frac{\Omega_{2n-1}^-(w)}{(1-w^2)^{2n}} - \frac{2}{(1-w^2)^{2n+1}}\left\{\Omega_{2n}^+(w)S_L + \Omega_{2n-1}^-(w) + \sum_{m=1}^{2n-1}\binom{2n}{m}\Omega_m^+(w)\Omega_{2n-m-1}^-(w)\right\}.\end{aligned} \quad \textbf{(31)}$$

Here, the $m=2n$ term (featuring a logarithmic function) and $m=0$ term have been partitioned from the rest of the sum. Although the first term sports a denominator with $1-w^2$ raised to an even power, one can use

$$\frac{\Omega_{2n-1}^-(w)}{(1-w^2)^{2n}} - \frac{2\Omega_{2n-1}^-(w)}{(1-w^2)^{2n+1}} = -\frac{(1+w^2)\Omega_{2n-1}^-(w)}{(1-w^2)^{2n+1}} \quad \textbf{(32)}$$

to have all denominators in the expression for D_{2n} be $(1-w^2)^{2n+1}$. If we introduce

$$\Lambda = \left(\frac{1+w^2}{w}\right)\log_e\left(\frac{1+w}{1-w}\right), \quad \textbf{(33)}$$

we have

$$D_{2n} = \frac{1}{(1-w^2)^{2n+1}}\left[-\frac{\Omega_{2n}^+(w)w\Lambda}{1+w^2} - (1+w^2)\Omega_{2n-1}^-(w) - 2\sum_{m=1}^{2n-1}\binom{2n}{m}\Omega_m^+(w)\Omega_{2n-m-1}^-(w)\right]. \quad \textbf{(34)}$$

The first term in brackets is a palindromic polynomial of w^2 of order $2n-2$ times $w^3\Lambda$, and the remaining terms combine to form w times a palindromic polynomial of w^2 of order $2n$.

For odd $p \geq -1$, this ensures that contributions to L_p and C_p arising from a term with $(2s+1)^{2n}$ in $f_{s,p}$ or $g_{s,p}$ will include a palindromic polynomial of w^2 of order $2n$ divided by $(1-w^2)^{2n+1}$. There is also a contribution to the numerators in C_p that is $w^2\Lambda$ times a palindromic polynomial of w^2 of order $2n-2$. Furthermore, if there are terms in which there are denominators having different powers of $1-w^2$, multiplying the numerator and denominator of each term by the appropriate even power of $1-w^2$ can establish one common denominator proportional to $(1-w^2)^{2p+7}$, with each numerator being either a palindromic polynomials of w^2 of order $2p+6$, or $w^2\Lambda$ times a palindromic polynomial of order $2p+4$ (or a polynomial of a lower order for which coefficients for powers $p+2\pm m$ are still equal). Combining terms therefore yields up to one term of each type.

For $p=-1$, we have

$$L_{-1} = -\frac{1-20w^2-90w^4-20w^6+w^8}{4\pi(1-w^2)^5} \quad \textbf{(35)}$$

and, separating effects of r_{-1},

$$C_{-1} = -\frac{L_{-1}r_{-1}}{2} - \frac{5w^8-112w^6-586w^4-112w^2+5}{6\pi(1-w^2)^5} + \frac{32w^4\Lambda}{\pi(1-w^2)^5}. \quad \textbf{(36)}$$

Besides remaining odd-order terms, similar methods show that the only even-order term is

$$C_0 = -\frac{1}{6}\sum_{s=0}^{\infty}(s^6+3s^5+s^4-3s^3-2s^2)w^{2s} = -\frac{24(w^8+3w^6+w^4)}{(1-w^2)^7}. \quad \textbf{(37)}$$

From Ref. [17], at small A we also have

$$F_X(A,w) = -\frac{96w^6(w^4+3w^2+1)}{(1-w^2)^7} + O(e^{-4\pi(w+1/w)A}), \quad \textbf{(38)}$$

which bears an uncanny resemblance to C_0.

B. Leading spectral terms

In the case of monochromatic radiation, Hankel's asymptotic expansion for Bessel functions of a large argument in Wolf's result leads to asymptotic expansions for $L_B(v,w)$ and $L_X(v,w)$. Equation (30) of Ref. [17] presents the leading terms for $L_B(v,w)$, for which the general expansion includes three types of terms with various inverse powers of v: non-oscillatory with odd powers, and oscillatory with $\cos(2v)$ times even powers or $\sin(2v)$ times odd powers. The expressions in Eq. (30) of Ref. [17] involve implicit functions of w labelled σ_n for $n=0,1,2,\ldots$, etc., which are defined in Eq. (28) of the same reference. Palindromic polynomials appear to all orders for every type of term in this expansion, which is proved in the next Section. From Ref. [17] we have

$$\begin{aligned} L_B(v,w) \sim \pi^{-1}[&A_1v^{-1}+C_2v^{-2}\cos(2v)+A_3v^{-3}+ \\ &S_3v^{-3}\sin(2v)+C_4v^{-4}\cos(2v)+\ldots]. \end{aligned} \quad \textbf{(39)}$$

Rearrangement of Eq. (30) of Ref. [17] gives

$$\left.\begin{aligned} A_1 &= 2/(1-w^2) \\ C_2 &= -1/(1-w^2) \\ A_3 &= (1-20w^2-90w^4-20w^6+w^8)/[4(1-w^2)^5] \\ S_3 &= -(1-18w^2+w^4)/[4(1-w^2)^3] \\ C_4 &= 3(3+20w^2+466w^4+20w^6+3w^8)/[32(1-w^2)^5] \end{aligned}\right\}. \quad \textbf{(40)}$$

From Wolf, the quantity $L_X(v,w)$ can be decomposed according to $g=(w+1/w)/2$ and

$$L_X(v,w) = (4w/v)[Y_1(v,w)\cos(vg)+Y_2(v,w)\sin(vg)]. \quad \textbf{(41)}$$

The Y_n-functions are defined by Wolf as well as in Ref. [17]. Using Hankel's asymptotic formula for Bessel functions of fixed order and large argument establishes the pattern for asymptotic expansions for both Y_n-functions: $v^{1/2}$ times either $s_\pm = \sin(v\pm\pi/4)$ divided by odd powers of v or $c_\pm = \cos(v\pm\pi/4)$ divided by even powers of v. Equations (65-66) of Ref. [17] present leading terms of

$$\begin{aligned} Y_1(v/w,w) &= +\frac{vw(1+w^2)}{2}\left(\frac{2}{\pi v}\right)^{1/2} \\ &[S_1^{(1)}s_-v^{-1}+C_2^{(1)}c_-v^{-2}+S_3^{(1)}s_-v^{-3}+\ldots] \end{aligned} \quad \textbf{(42)}$$

and

$$\begin{aligned} Y_2(v/w,w) &= -\frac{vw^2}{2}\left(\frac{2}{\pi v}\right)^{1/2} \\ &[S_1^{(2)}s_+v^{-1}+C_2^{(2)}c_+v^{-2}+S_3^{(2)}s_+v^{-3}+\ldots]. \end{aligned} \quad \textbf{(43)}$$

The leading coefficients of these can be re-expressed in a simpler form than was given previously, giving

$$\left.\begin{aligned} S_1^{(1)} &= 2/(1-w^2)^2 \\ C_2^{(1)} &= 3(1+30w^2+w^4)/[4(1-w^2)^4] \\ S_3^{(1)} &= \frac{15(1-196w^2-1658w^4-196w^6+w^8)}{64(1-w^2)^6} \end{aligned}\right\} \quad \textbf{(44)}$$

and

$$\left.\begin{aligned} S_1^{(2)} &= 4/(1-w^2)^2 \\ C_2^{(2)} &= 3(5+22w^2+5w^4)/[2(1-w^2)^4] \\ S_3^{(2)} &= -\frac{15(7+420w^2+1194w^4+420w^6+7w^8)}{32(1-w^2)^6} \end{aligned}\right\}. \quad \textbf{(45)}$$

Palindromic polynomials appear in every term to all orders, a fact that is proven later.

4. EXACT EVALUATION OF MAIN EFFECTS

A. Preliminary Considerations

Equations (21) and (22) of Ref. [17] provide exact integral representations of $L_B(v,w)$ and $F_B(A,w)$. To evaluate these integrals, we introduce the shorthand,

$$D(a,w)=\frac{1}{(2\pi)^2}\int_{-\pi}^{+\pi}d\theta\int_{-\pi}^{+\pi}d\theta'\,G(\theta,\theta';w)\,\delta(c-c'-2a). \qquad \textbf{(46)}$$

Here we have $h=\exp[i(\theta+\theta')/2]$, $\eta=\exp[i(\theta-\theta')]$, $w_1^{\pm}=we^{\pm i\theta}$, $w_2^{\pm}=we^{\mp i\theta'}$, $c=\cos\theta$, $c'=\cos\theta'$, $s=\sin\theta$, $s'=\sin\theta'$, $\alpha=e^{i\theta/2}$, $\beta=e^{-i\theta'/2}$,

$$\Lambda_i^{\pm}=\frac{1}{2w_i^{\pm}}\log_e\left(\frac{1+w_i^{\pm}}{1-w_i^{\pm}}\right) \qquad \textbf{(47)}$$

and

$$G(\theta,\theta';w)=(1+\eta)\left(\frac{h\Lambda_1^{+}-h^{-1}\Lambda_2^{+}}{h-h^{-1}}\right). \qquad \textbf{(48)}$$

(Unless necessary for clarity, we suppress several dependences.) Symmetric ranges of integration and invariance of the integrand with respect to the exchange $\theta\leftrightarrow-\theta'$ imply

$$L_B(v,w)=4\int_0^1 da\,\cos(2av)D(a,w) \qquad \textbf{(49)}$$

and

$$F_B(A,w)=12\int_0^1 da\,S(A,2a)D(a,w). \qquad \textbf{(50)}$$

These formulas account for the fact that the boundary-diffraction wave portion of light passing from a point on the source to any given point on the detector plane would have taken a superposition of two-segment paths, but $D(a,w)$ expresses the effects of the associated distribution functions for path-length differences integrated over a detector area. In this sense, it is an aggregate path-length-difference weighting function. The absolute difference between any two such path lengths cannot be negative and cannot exceed a value corresponding to $\lambda v/\pi$ in classical notation. Reference [17] and the Appendix discuss the function $S(A,l)$, which helps account for cumulative interference effects in the case of a Planck source. The Appendix also discusses Mellin transforms of $S(A,l)$, $S(A,l)+l^{-4}$, $S(A,l)\log_e l$ and $[S(A,l)+l^{-4}]\log_e l$ relevant for evaluating $F_B(A,w)$.

Regarding $D(a,w)$, one may change the ranges of integration to have

$$\begin{aligned}D(a,w)&=\frac{1}{(2\pi)^2}\int_0^{\pi}d\theta\int_0^{\pi}d\theta'\\&\left[(1+\alpha^2\beta^2)\left(\frac{\alpha\beta^{-1}\Lambda_1^{+}-\beta\alpha^{-1}\Lambda_2^{+}}{\alpha\beta^{-1}-\beta\alpha^{-1}}\right)+\ldots\right]\delta(c-c'-2a).\end{aligned} \qquad \textbf{(51)}$$

Three terms indicated but not shown in square brackets are obtained from the term shown if one changes the sign(s) of θ (thereby inverting α and replacing Λ_1^{+} with Λ_1^{-}), and/or θ' (thereby inverting β and replacing Λ_2^{+} with Λ_2^{-}). The sum of all four terms can be written with a common denominator that is

$$(\alpha\beta^{-1}-\beta\alpha^{-1})\cdots(\alpha^{-1}\beta-\beta^{-1}\alpha)=4(c-c')^2=16a^2 \qquad \textbf{(52)}$$

and can be taken outside the integral. Simplifying the resulting coefficients of Λ_1^{+}, Λ_1^{-}, Λ_2^{+} and Λ_2^{-} gives

$$\begin{aligned}D(a,w)&=\frac{i}{(2\pi)^2a}\int_0^{\pi}d\theta\int_0^{\pi}d\theta'\\&[e^{i\theta}c's\Lambda_1^{+}-e^{-i\theta}c's\Lambda_1^{-}+e^{-i\theta'}cs'\Lambda_2^{+}-e^{i\theta'}cs'\Lambda_2^{-}]\\&\delta(c-c'-2a)\\&=\frac{i}{(2\pi)^2a}\int_{-1}^{+1}dc\int_{-1}^{+1}dc'\,[e^{i\theta}c's\Lambda_1^{+}-\ldots]\left(\frac{\delta(c-c'-2a)}{ss'}\right).\end{aligned} \qquad \textbf{(53)}$$

One may rewrite this using only one variable of integration, x, related to c and c' by $c=(1-a)x+a$ and $c'=(1-a)x-a$, and rewrite the denominator using

$$(ss')^2=(1-a)^2(1+a)^2R^2 \qquad \textbf{(54)}$$

with $k=-(1-a)/(1+a)$ and $R=[(1-x^2)(1-k^2x^2)]^{1/2}$. This gives

$$D(a,w)=\frac{i}{(2\pi)^2a(1+a)}\int_{-1}^{+1}dx\,[e^{i\theta}c's\Lambda_1^{+}-\ldots]/R. \qquad \textbf{(55)}$$

With one additional level of differentiation and integration, according to

$$\begin{aligned}D(a,w)&=\frac{i}{2w(2\pi)^2a(1+a)}\\&\int_{-1}^{+1}\frac{dx}{R}\int_0^{w}d\omega\frac{d}{d\omega}[2\omega(e^{i\theta}c's\Lambda_1^{+}(\omega)-\ldots)],\end{aligned} \qquad \textbf{(56)}$$

terms that contained logarithmic functions become ones with algebraic functions. We may regroup this to have one term with a denominator involving s and one term with a denominator involving s'. If we introduce a function that is even with respect to x,

$$\begin{aligned}g(\omega,a,x^2)&=\frac{cs'^2}{(1-\omega^2)^2+4\omega^2s'^2}-\frac{c's^2}{(1-\omega^2)^2+4\omega^2s^2}\\&=\frac{c(1-c'^2)}{(1+\omega^2)^2-4\omega^2c'^2}-\frac{c'(1-c^2)}{(1+\omega^2)^2-4\omega^2c^2},\end{aligned} \qquad \textbf{(57)}$$

we have (with $h_0=1-w^2$)

$$\begin{aligned}D(a,w)&=\frac{4}{w(2\pi)^2a(1+a)}\int_0^{+1}\frac{dx}{R}\int_0^{w}d\omega\,(1+\omega^2)g(\omega,a,x^2)\\&=\frac{i}{w(2\pi)^2a(1+a)}\\&\int_0^{1}\frac{dx}{R}\left[c's\log_e\left(\frac{h_0+2iws}{h_0-2iws}\right)-cs'\log_e\left(\frac{h_0+2iws'}{h_0-2iws'}\right)\right].\end{aligned} \qquad \textbf{(58)}$$

Real a implies $i\log_e[(h_0+2iws)/(h_0-2iws)]=-2\tan^{-1}(2ws/h_0)$, etc. For complex a, s is the branch of $(1-c^2)^{1/2}$ that is positive for $1-c^2>0$ and has a branch cut for $1-c^2<0$, and similarly for s', and the logarithm functions are real for positive argument and have a branch cut where the argument is negative.

Equations (49-50) initially consider $0 < a < 1$, but it is helpful to analytically continue $D(a,w)$ away from the real-a axis while only considering real w. The integrand in Eq. (58) is a linear combination of terms of the form $c's^{2n} - cs'^{2n} = c'(1-c^2)^n - c(1-c'^2)^n$. $D(a,w)$ is therefore a linear combination of terms of the form

$$
\begin{aligned}
S_{pq} &= \frac{(1-a)^{2p} a^{2q}}{1+a} \int_0^1 dx\, x^{2p} / R \\
&= \left(\frac{\Gamma(1/2)\Gamma(p+1/2)}{2\Gamma(p+1)} \right) \frac{(1-a)^{2p} a^{2q}}{1+a} F\left(p+\frac{1}{2}, \frac{1}{2}; p+1; k^2 \right) \\
&= \left(\frac{\Gamma(1/2)\Gamma(p+1/2)}{2\Gamma(p+1)} \right) \frac{(1-a)^{2p} a^{2q} (1-k)^{-2p-1}}{1+a} \\
&\quad F\left(p+\frac{1}{2}, p+\frac{1}{2}; 2p+1; -\frac{4k}{(1-k)^2} \right).
\end{aligned}
\tag{59}
$$

Here F is a hypergeometric function and the last step uses a quadratic transformation of variables. With $k = -(1-a)/(1+a)$, we have $1-k = 2/(1+a)$ and $-4k/(1-k)^2 = 1-a^2$. A linear transformation of variables simplifies this to

$$
\begin{aligned}
S_{pq} &\sim \frac{(1-a^2)^{2p} a^{2q}}{2} \\
&\sum_{n=0}^{\infty} \frac{[(p+1/2)_n]^2}{n!(1)_n} [\psi(n+1) - \psi(n+p+1/2) - \log_e a] a^{2n}
\end{aligned}
\tag{60}
$$

so that at small a one has

$$
D(a,w) \sim \textstyle\sum_{n=0}^{\infty} (c_{2n} a^{2n} + l_{2n} a^{2n} \log_e a). \tag{61}
$$

The form of $L_B(v,w)$ also supports such an expansion with even powers only. For, suppose one decomposes the $\cos(2av)$ in the integral representation of $L_B(v,w)$ given in Eq. (49) into a combination of integrals involving $\exp(+2iav)$ and $\exp(-2iav)$ and deforms the contours of integration to run respectively from zero to $\pm i\infty$, to $\pm i\infty + 1$, and to 1. One then obtains contributions to $L_B(v,w)$ with exponentially damped integrands with complex phases that are very nearly zero or $\pm 2v \bmod \pi/2$. Terms featured in the asymptotic expansion for $L_B(v,w)$ indicate even powers of a near $a = 0$.

Suppose that one introduces partitions of $D(a,w)$, $S(A,2a)$ and the integral of their product related to $F_B(A,w)$, according to

$$
D(a,w) = D_L(a,w) + D_R(a,w) \tag{62}
$$

with

$$
D_L(a,w) = c_0 + c_2 a^2 + (l_0 + l_2 a^2) \log_e a, \tag{63}
$$

as well as

$$
S(A,2a) = [S(A,2a) + (2a)^{-4}] - (2a)^{-4} \tag{64}
$$

and

$$
\begin{aligned}
&\int_0^1 da\, D(a,w) S(A,2a) = \int_0^\infty da\, D_L(a,w)\, S(A,2a) \\
&+ \int_1^\infty da\, D_L(a,w)\, (2a)^{-4} - \int_0^1 da\, D_R(a,w)\, (2a)^{-4} \\
&- \int_1^\infty da\, D_L(a,w)\, [S(A,2a) + (2a)^{-4}] \\
&+ \int_0^1 da\, D_R(a,w)\, [S(A,2a) + (2a)^{-4}].
\end{aligned}
\tag{65}
$$

Relating this to $F_B(A,w)$ through Eq. (50) furnishes insight. The first integral accounts for the C_{-3}, C_{-1} and L_{-1} terms, integrals involving $(2a)^{-4}$ alone are independent of A and account for the C_0 term, whereas the integrals involving $S(A,2a) + (2a)^{-4}$ vanish at small A because we have $S(A,2a) \sim -(2a)^{-4} + O(e^{-4\pi a/A})$. The integral involving $D_L(a,w)$ and $S(A,2a) + (2a)^{-4}$ vanishes as $O(e^{-4\pi/A})$ at sufficiently small A, whereas the integral involving $D_R(a,w)$ and $S(A,2a) + (2a)^{-4}$ accounts for all remaining contributions to $F_B(A,w)$ that do not vanish similarly. Furthermore, its upper limit of integration can be reduced to only a few times A with little consequence. If the upper limit is a' instead of unity, the error incurred is only $O(e^{-4\pi a'/A})$.

The leading term of $F_B(A,w)$ and the Mellin transform of $S(A,l)\log_e l$ confirm $l_0 = -2/[\pi^2(1-w^2)]$. The Mellin transform of $S(A,l)$ vanishes for Mellin exponent $2n = 0$, precluding insight into the value of c_0, but analysis of Eq. (58) yields the same value for l_0 and $c_0 = -l_0(2\log_e 2 + 1 - \Lambda)$. Relating A^{-1} terms in $F_B(A,w)$ to the Mellin transforms of $S(A,l)$ and $S(A,l)\log_e l$ for $2n = 2$ gives $l_2 = -2L_{-1}/\pi$ and $c_2 = [(3 - 2\gamma - 2\log_e 2)L_{-1} - 2C_{-1}]/\pi$. For $n > 1$ Mellin transforms of the short-ranged functions $S(A,l) + l^{-4}$ and $[S(A,l) + l^{-4}]\log_e l$ imply (see Appendix) $l_{2n} = L_{2n-3}/[12\chi(2n)]$ and $c_{2n} = \{C_{2n-3} - [\xi(2n) - \log_e 2]L_{2n-3}\}/[12\chi(2n)]$. This ensures connections between leading terms or pairs thereof in the power series expansion of $D(a,w)$ about $a = 0$, leading terms in $F_B(A,w)$ at small A, and non-oscillatory terms in $L_B(v,w)$, establishing there also being palindromic polynomials in the latter.

There are likewise connections between terms in the Taylor expansion of $D(a,w)$ about $a = 1$ and oscillatory terms in $L_B(v,w)$. For $a = 1 + \varepsilon$ and $\varepsilon \to 0$, k and $D(a,w)$ both vanish, and one has $D(a,w) = -\varepsilon/[\pi(1-w^2)] + O(\varepsilon^2)$. For any given appearance of $c's^{2n}$ or cs'^{2n} in the integrand in Eq. (58), there is a multiplier, $w^{2n-1}/(1-w^2)^{2n-1}$. With $1 - c = (1-a)(1-x)$ and $1 + c' = (1-a)(1+x)$, s^{2n} and s'^{2n} contain a factor $(1-a)^n$. This ensures that, when integrating from $a = 1$ to $a = 1 \pm i\infty$, contributions to coefficients of type C_{q+1} or S_{q+1} in Eq. (39) can only involve terms with $n \le q$, having the form

$$\left.\begin{aligned} C_{q+1} &= \frac{\alpha_1}{1-w^2} + \ldots + \frac{\alpha_q w^{2q-2}}{(1-w^2)^{2q-1}} \\ S_{q+1} &= \frac{\beta_1}{1-w^2} + \ldots + \frac{\beta_q w^{2q-2}}{(1-w^2)^{2q-1}} \end{aligned}\right\}. \quad \textbf{(66)}$$

When expressed with a common denominator of $(1-w^2)^{2q-1}$, the numerators in these coefficients are always palindromic polynomials.

B. Numerical Evaluation of D-function

Regarding evaluation of the aggregate path-length difference weighting function $D(a,w)$, we shall first consider having $w<0.9$. Here we note that Eq. (58) suggests that having $|a|/(1-w^2)^2$ appropriately bounded ensures convergence of the first several terms of Eq. (61) to an accurate result. For $|a|<0.01(1-w^2)^2$, therefore, we use Eq. (61) and include terms through $c_{12}a^{12}+l_{12}a^{12}\log_e a$ with the coefficients evaluated as described in Section 3.

We also have demonstrated an algorithmically simpler method of evaluation which is as follows. First set $a_0=0.01(1-w^2)^2$ and evaluate $D(a,w)$ at $a=a_0e^{i\alpha}$ for representative $0<\alpha<\pi$ and use $D(a^*,w)=[D(a,w)]^*$. Fourier analysis yields leading coefficients according to

$$\left.\begin{aligned} &\sum_{n=0}^{\infty} l_{2n}a_0^{2n}\exp(2in\alpha) = \Delta(a,w) \\ &\sum_{n=0}^{\infty} c_{2n}a_0^{2n}\exp(2in\alpha) = D(a,w) - \Delta(a,w)\log_e a \end{aligned}\right\} \quad \textbf{(67)}$$

with $\Delta(a,w)=[D(a,w)-D(ae^{-i\pi},w)]/(i\pi)$. To evaluate each value of $D(a,w)$ we use Eq. (58) with integration over $\varphi=\cos^{-1}x$, with 128 Gauss-Legendre quadrature points for $0<\varphi<|8a|^{1/2}$ and for $|8a|^{1/2}<\varphi<\pi/2$. For the Fourier analysis, we use $\alpha/\pi=1/14, 3/14, \ldots, 13/14$. Concentration of quadrature points at small φ accounts for R passing near zero for $\alpha\approx\pm\pi$. This has yielded a relative accuracy of 10^{-12} for $D(a,w)$. For $|a|>0.01(1-w^2)^2$ the same quadrature can be used equally well.

Having larger values of w (and/or treating $|\alpha|>13\pi/14$) can require enhanced quadrature. It would be unusual in practical radiometry to have a much larger value of w, because that would imply having shadow boundaries near the edges of optical surfaces. Moreover, it is unlikely that so much attention would be warranted for sufficiently small values of a, because leading terms in $L_B(v,w)$ and $F_B(A,w)$ would already give accurate results.

C. Numerical Evaluation for Planck (thermal) case

If A is sufficiently small, one can use

$$\begin{aligned} F_B(A,w) &= C_{-3}A^{-3} + C_{-1}A^{-1} + L_{-1}A^{-1}\log_e A + C_0 \\ &+12\int_0^{a'} da\,[S(A,2a)+(2a)^{-4}]\,D_R(a,w) \\ &-12\int_1^{\infty} da\,[S(A,2a)+(2a)^{-4}]\,D_L(a,w) + O(e^{-4\pi a'/A}). \end{aligned} \quad \textbf{(68)}$$

Note that a' does not need to be much larger than A and should never exceed unity. By partitioning $D_R(a,w)$ into terms with or without logarithms at small a, e.g., $a<\min(0.01(1-w^2)^2, A)$, one can integrate each portion of $S(A,2a)D_R(a,w)$ by quadrature using suitable points and weights. One can use Gauss-Legendre quadrature integration of $S(A,2a)D_R(a,w)$ for the remainder of its range of integration and that of the exponentially damped $-[S(A,2a)+(2a)^{-4}]D_L(a,w)$ outward from $a=1$. If A is larger, one can simply integrate $S(A,2a)D(a,w)$ over $0<a<1$:

$$\begin{aligned} F_B(A,w) &= 6\int_0^{\pi} d\varphi\sin\varphi\, D(a,w)\, S(A,2a) \\ &= \frac{\pi^4}{15A^4} - \frac{2\pi^6}{63A^6} + \\ &6\int_0^{\pi} d\varphi\sin\varphi\, D(a,w)\left[S(A,2a) - \frac{\pi^4}{45A^4} + \frac{16\pi^6a^2}{189A^6}\right]. \end{aligned} \quad \textbf{(69)}$$

The change of variable of integration to φ with $a=(1+\cos\varphi)/2$ and extraction of effects of the leading terms of $S(A,2a)$ from the integral accelerate the quadrature's convergence. For $w\le 0.9$, we achieved accuracy in $F_B(A,w)$ that was $\sim 10^{-10}$ times $F(A,w)$ using 128 Gauss-Legendre quadrature points in the integrals in Eq. (68) for $A<0.015$ and the integral in Eq. (69) for $A>0.015$.

D. Numerical Evaluation for spectral case

For small v one can likewise evaluate $L_B(v,w)$ according to Eq. (49) using numerical quadrature. On the other hand, when evaluating $L_B(v,w)$ exactly for large v, it has proved useful to decompose it into its non-oscillatory part and oscillatory parts that have phase factors e^{2iv} and e^{-2iv}. This is achieved by rewriting Eq. (49) as follows:

$$\begin{aligned} &L_B(v,w) = \\ &\frac{2}{v}\Re\left[\left(i\int_0^{\infty} dt\, e^{-t}D(it/(2v),w)\right) - ie^{2iv}\int_0^{\infty} dt\, e^{-t}D(1+it/(2v),w)\right] \\ &= L_{\text{n.o.}}(v,w) + e^{2iv}L_+(v,w) + e^{-2iv}[L_+(v,w)]^*. \end{aligned} \quad \textbf{(70)}$$

The advantage of this form is particularly clear when one is to incorporate the above result into Eq. (3) to treat extended sources, a task that can be accelerated greatly by appropriate use of contour of integration in Eq. (3). The two integrals in Eq. (70) are readily evaluated using Gauss-Laguerre quadrature. They are smooth functions of v, a property that allows their evaluation over a range of values of v for fixed u as in Eq. (3) based on evaluation at a few discrete values of v and Chebyshev-Lagrange interpolation.

5. NUMERICAL EVALUATION OF REMAINING EFFECTS

Equations (64) and (62) of Ref. [17] provide integral representations for numerical evaluation of the interference terms $F_X(A,w)$ and $L_X(v,w)$ when the leading asymptotic terms do not suffice. Thus, if Eq. (38) of this work is not sufficiently accurate, one can evaluate $F_X(A,w)$ using quadrature integration; here 128-point Gauss-Legendre quadrature or Eq. (38) could ensure an accuracy $\sim 10^{-11}F(A,w)$ for $w<0.9$. To obtain $L_X(v,w)$, one may first decompose the expression in Eq. (62) of Ref. [17] into two exponentials, according to $L_X(v,w)=L_X^{(+)}(v,w)+L_X^{(-)}(v,w)$, with

$$L_X^{(\pm)}(v,w)=\frac{2w^2}{\pi}\int_{-1}^{+1}dx\frac{(1-x^2)^{1/2}\exp[\pm iv(x-g)]}{1+w^2-2wx}. \tag{71}$$

Gauss-Chebyshev quadrature permits evaluation for small v, while contour integration helps for large v, according to

$$\begin{aligned} &L_X^{(+)}(v,w)\\ &=\frac{2w^2}{\pi}\left(\int_{-1}^{-1+i\infty}dx-\int_{+1}^{+1+i\infty}dx\right)\frac{(1-x^2)^{1/2}e^{iv(x-g)}}{1+w^2-2wx}\\ &=e^{-i\phi_1(v)}Q_1(u,v)+e^{-i\phi_2(v)}Q_2(u,v),\end{aligned} \tag{72}$$

with $\phi_1(v)=(u+v)^2/(2u)$, $\phi_2(v)=(u-v)^2/(2u)$, and

$$\left.\begin{aligned} Q_1(u,v)&=+\frac{4iv^{1/2}}{\pi}\int_0^\infty\frac{ds\, s^2e^{-s^2}[(+i)(2-is^2/v)]^{1/2}}{(u+v)^2-2ius^2}\\ Q_2(u,v)&=-\frac{4iv^{1/2}}{\pi}\int_0^\infty\frac{ds\, s^2e^{-s^2}[(-i)(2+is^2/v)]^{1/2}}{(u-v)^2-2ius^2}\end{aligned}\right\} \tag{73}$$

and likewise for $L_X^{(-)}(v,w)$. The last integrals are amenable to Gauss-Hermite quadrature and are also smooth functions of v amenable to interpolation schemes. This decomposition also proves helpful when applying Eq. (3) to treat extended sources. Note that one also has

$$\begin{aligned} L_X(v,w)&=\frac{4w^2}{\pi}\int_{-1}^{+1}dx\sqrt{1-x^2}\,\frac{\cos(vx-vg)}{1+w^2-2wx}\\ &=\frac{4w^2}{\pi}[\cos(vg)I_c+\sin(vg)I_s],\end{aligned} \tag{74}$$

with

$$\begin{aligned} I_c&=\int_{-1}^{+1}dx\sqrt{1-x^2}\left(\frac{\cos(vx)}{1+w^2-2wx}\right)\\ &=(1+w^2)\int_{-1}^{+1}dx\sqrt{1-x^2}\left(\frac{\cos(vx)}{(1+w^2)^2-4w^2x^2}\right)\\ &=(1+w^2)\int_{-1}^{+1}dx\sqrt{1-x^2}\left(\frac{\cos(vx)}{(1-w^2)^2+4w^2(1-x^2)}\right)\end{aligned} \tag{75}$$

and

$$\begin{aligned} I_s&=\int_{-1}^{+1}dx\sqrt{1-x^2}\left(\frac{\sin(vx)}{1+w^2-2wx}\right)\\ &=2w\int_{-1}^{+1}dx\sqrt{1-x^2}\left(\frac{x\sin(vx)}{(1+w^2)^2-4w^2x^2}\right)\\ &=2w\int_{-1}^{+1}dx\sqrt{1-x^2}\left(\frac{x\sin(vx)}{(1-w^2)^2+4w^2(1-x^2)}\right).\end{aligned} \tag{76}$$

These two integrals are proportional to Y_1 and Y_2 and give insight into their asymptotic properties. It is first helpful to note

$$\frac{1}{(1-w^2)^2+4w^2(1-x^2)}=\frac{1}{(1-w^2)^2}-\frac{4w^2(1-x^2)}{(1-w^2)^4}+\ldots \tag{77}$$

Suppose one decomposes $\cos(vx)$ and $\sin(vx)$ into terms involving $e^{\pm ivx}$ and integrates contributions of each exponential from -1 to $-1\pm i\infty$ and from $+1\pm i\infty$ to $+1$. Contributions involving $(4w^2)^n/(1-w^2)^{2n+2}$ have expansions with denominators proportional to $v^{n'+3/2}$ with $n'>n$, the leading power being determined by the factor $[x-(\pm1)]^{n+1/2}$ in $(1-x^2)^{n+1/2}$ near $x=\pm1$, and higher n' values arising because of expansion of the other factor, $[x+(\pm1)]^{n+1/2}$, about $x=\pm1$. If all terms with each value of n' are combined with a common denominator, $(1-w^2)^{2n'+2}$, the numerator would be a palindromic polynomial of w^2.

6. GENERALIZATION TO EXTENDED SOURCES

It is straightforward to perform the integration in Eq. (3) for $F_B(A,w)$, $F_X(A,w)$ and the non-oscillatory part of $L_B(v,w)$ numerically via Gauss-Chebyshev quadrature. This is also true for the oscillatory parts of $L_B(v,w)$ and $L_X(v,w)$ if the argument of the complex exponential varies sufficiently slowly, although extended Gauss-Legendre quadrature over $\cos^{-1}x$ may accelerate convergence. In other instances, one can eliminate highly oscillatory integrands by deforming the contour of integration in Eq. (3), in a manner suitable for the phase factor of each term, making it decay instead of oscillate.

For contributions from $L_+(v,w)$, deforming the integration so that x runs from -1 to $-1\pm i\infty$ and from $+1\pm i\infty$ to $+1$ achieves this; one can avoid awkwardness of the integrand by changing the variable of integration along each vertical contour to t with $\Im x=\pm t^2/(2v_0\sigma)$ and using Gauss-Hermite quadrature. One can estimate contributions to $L_+(v,w)$ beyond those found in Eq. (39) by Chebyshev-Lagrange interpolation [18] after sampling $L_+(v,w)$ at N points in the range from $v=v_-=v_0(1-\sigma)$ to $v=v_+=v_0(1+\sigma)$, according to $v_k=v_0(1+\sigma\cos\theta_k)\equiv v_0(1+\sigma x_k)$ with $\theta_k=\pi(k-1/2)/N$ and $k=1,\ldots,N$. This necessitates evaluating $L_+(v,w)$ for values slightly outside of the range, $v_-<v<v_+$, but having only real sampled values of v_k also ensures evaluating $D(a,w)$ only for real values of w. With (complex) $v=v_0(1+\sigma\cos\theta)\equiv v_0(1+\sigma x)$, one has

$$L_+(v,w(v,u))\approx\sum_{k=1}^N\alpha_k(x)\,L_+(v_k,w(v_k,u)) \tag{78}$$

with

$$\alpha_k(x)=\frac{T_N(x)T_{N-1}(x_k)}{N(x-x_k)}=\prod_{k'\neq k}\left(\frac{x_{k'}-x}{x_{k'}-x_k}\right). \tag{79}$$

The first form can be numerically expedient given a large number of sampling points, and the second form helps for $x\to x_k$.

Quadratic exponents in phase factors in Eq. (73) suggest adapting Eq. (3) to integrate along hyperbolic contours. Introducing $M(v,v_0)=G(\sigma,x)/(v_0\sigma)$ implies

$$\begin{aligned} &\int_{-1}^{+1}dx\,G(\sigma,x)\,L_X(v_0(1+\sigma x),w)\\ &=2\Re\int_{v_-}^{v_+}dv\,M(v,v_0)\,L_X^{(+)}(v,w).\end{aligned} \tag{80}$$

The latter can be rewritten using

$$\begin{aligned} &\int_{v_-}^{v_+}dv\,M(v,v_0)\,L_X^{(+)}(v,w)\\ &=\sum_{\mu=1,2}\left(\int_{C_{\mu,-}}dv-\int_{C_{\mu,+}}dv\right)M(v,v_0)e^{-i\phi_\mu(v)}Q_\mu(u,v)\end{aligned} \tag{81}$$

On $C_{1,\pm}$ one has $v=[(u+v_\pm)^2-2iut^2]^{1/2}-u$ and $(u+v)^2=(u+v_\pm)^2-2iut^2$, and on $C_{2,\pm}$ one has $v=u-[(u-v_\pm)^2-2iut^2]^{1/2}$ and $(u-v)^2=(u-v_\pm)^2-2iut^2$. The parameter t runs from 0 to $+\infty$, and phase factors are constants (to be taken outside of the integral) times $\exp(-t^2)$, making integration amenable to Gauss-Hermite quadrature.

The preponderance of extended sources in practical radiometry motivates closed-form formulas for leading-order diffraction effects. With the change of variable in Eq. (3) from x to

$$y=2\left[\frac{(1+\sigma x)^2-(1-\sigma)^2}{(1+\sigma)^2-(1-\sigma)^2}\right]-1 \quad \textbf{(82)}$$

one has $y=\pm 1$ at $x=\pm 1$, $dy=(1+\sigma x)dx$, and, for any function f,

$$\frac{1}{\pi}\int_{-1}^{+1}dxG(\sigma,x)f(1+\sigma x)=\frac{2}{\pi}\int_{-1}^{+1}dy\left(\frac{\sqrt{1-y^2}}{q}\right)f(q^{1/2}) \quad \textbf{(83)}$$

with $q=1+\sigma^2+2\sigma y=(1+\sigma x)^2$. A limiting case has $f(q^{1/2})=1-2/[\pi v_0 q^{1/2}(1-w_0^2/q)]+\ldots$, with $w_0^2=(u/v_0)^2$. The ratio of the actual flux Φ_L to the geometrically expected flux Φ_0 is

$$\frac{\Phi_L}{\Phi_0}\approx 1-\frac{4}{\pi^2 v_0}\int_{-1}^{+1}\frac{dy\sqrt{1-y^2}}{q^{3/2}(1-w_0^2/q)}. \quad \textbf{(84)}$$

A non-limiting case has $f(q^{1/2})=q\{1+2/[\pi v_0 q^{1/2}(1-w_0^2 q)]+\ldots\}$, with $w_0^2=(v_0/u)^2$, so the ratio of the actual flux Φ_{NL} to the geometrically expected flux is

$$\frac{\Phi_{NL}}{\Phi_0}\approx 1+\frac{4}{\pi^2 v_0}\int_{-1}^{+1}\frac{dy\sqrt{1-y^2}}{q^{1/2}(1-w_0^2 q)}. \quad \textbf{(85)}$$

Ratios affecting total power Planck sources have the replacement $v_0^{-1}\to\zeta(3)A_0/[3\zeta(4)]$. If desired, integration by Chebyshev quadrature is still trivial for the above expressions.

It is instructive to expand the integrands in successive powers of w_0^2 and integrate. A limiting case ensures $w_0^2/q<1$, giving

$$\frac{\Phi_\mathrm{L}}{\Phi_0}\approx 1-\frac{2}{\pi v_0}\sum_{s=0}^{\infty}w_0^{2s}F\left(\frac{3}{2}+s,\frac{1}{2}+s;2;\sigma^2\right); \quad \textbf{(86)}$$

and a non-limiting case ensures $w_0^2 q<1$, giving

$$\frac{\Phi_\mathrm{NL}}{\Phi_0}\approx 1+\frac{2}{\pi v_0}\sum_{s=0}^{\infty}w_0^{2s}F\left(\frac{1}{2}-s,-\frac{1}{2}-s;2;\sigma^2\right). \quad \textbf{(87)}$$

With $\omega=w_0(1-\sigma^2)$, a linear transformation of variable gives

$$\frac{\Phi_\mathrm{NL}}{\Phi_0}\approx 1+\frac{2}{\pi v_0}(1-\sigma^2)^2\sum_{s=0}^{\infty}\omega^{2s}F\left(\frac{5}{2}+s,\frac{3}{2}+s;2;\sigma^2\right). \quad \textbf{(88)}$$

One can rewrite the summands in Eq. (86-87) as even functions of $(2s+1)$ plus odd functions of $(2s+1)$. Summing even or odd contributions over s at each order in σ^2 gives a result that features palindromic polynomials to all orders, which is

$$\begin{aligned}\varepsilon_E(v_0,w_0,\sigma)&=\frac{1}{(1-w_0^2)}+\frac{\sigma^2}{8}\left(\frac{1+6w_0^2+w_0^4}{(1-w_0^2)^3}\right)+\\&\frac{\sigma^4}{64}\left(\frac{7+52w_0^2+10w_0^4+52w_0^6+7w_0^8}{(1-w_0^2)^5}\right)+\ldots\end{aligned} \quad \textbf{(89)}$$

or

$$\begin{aligned}&\varepsilon_O(v_0,w_0,\sigma)=(1+w_0^2)\\&\left[\frac{\sigma^2}{4(1-w_0^2)^2}+\frac{\sigma^4}{8}\left(\frac{1+6w_0^2+w_0^4}{(1-w_0^2)^4}\right)+\ldots\right]\end{aligned} \quad \textbf{(90)}$$

respectively, and we have

$$\left.\begin{aligned}\frac{\Phi_\mathrm{L}}{\Phi_0}&\approx 1-\frac{2}{\pi v_0}\left[\varepsilon_E(v_0,w_0,\sigma)+\varepsilon_O(v_0,w_0,\sigma)\right]\\\frac{\Phi_\mathrm{NL}}{\Phi_0}&\approx 1+\frac{2}{\pi v_0}\left[\varepsilon_E(v_0,w_0,\sigma)-\varepsilon_O(v_0,w_0,\sigma)\right]\end{aligned}\right\}. \quad \textbf{(91)}$$

For small w_0^2, expanding in its powers may be preferred. With $F_s(\sigma)=F(3/2+s,1/2+s;2;\sigma^2)$, we have $F_0(\sigma)=(4/\pi)D(\sigma)$ and $F_1(\sigma)=\{4/[3\pi(1-\sigma^2)^2]\}[2K(\sigma)-(1+\sigma^2)D(\sigma)]$, and properties of contiguous hypergeometric functions give

$$(2s+3)(1-\sigma^2)^2F_{s+1}(\sigma)=4s(1+\sigma^2)F_s(\sigma)-(2s-3)F_{s-1}(\sigma). \quad \textbf{(92)}$$

One can therefore introduce $m_s^{(D)}(\sigma^2)$ and $m_s^{(K)}(\sigma^2)$ to have

$$F_s(\sigma)=\frac{4}{\pi}\left(\frac{m_s^{(D)}(\sigma^2)D(\sigma)+m_s^{(K)}(\sigma^2)K(\sigma)}{(2s+1)!!\,(1-\sigma^2)^{2s}}\right) \quad \textbf{(93)}$$

with the recurrence relation

$$\begin{aligned}&m_{s+1}^{(K,D)}(\sigma^2)=4s(1+\sigma^2)m_s^{(K,D)}(\sigma^2)-\\&(2s-3)(2s+1)(1-\sigma^2)^2m_{s-1}^{(K,D)}(\sigma^2).\end{aligned} \quad \textbf{(94)}$$

For all $s\geq 0$, $m_s^{(K)}(\sigma^2)$ and $m_s^{(D)}(\sigma^2)$ are palindromic polynomials of order $s-1$ and s, respectively, with $m_0^{(K)}(\sigma^2)=0$, $m_0^{(D)}(\sigma^2)=1$, $m_1^{(K)}(\sigma^2)=2$, and $m_1^{(D)}(\sigma^2)=-(1+\sigma^2)$. One may introduce

$$X_{(K,D)}(w,\sigma)\sim\sum_{s=0}^{\infty}\frac{m_{s+1}^{(K,D)}(\sigma^2)}{(2s+3)!!}\frac{w^{2s}}{(1-\sigma^2)^{2s+2}}, \quad \textbf{(95)}$$

which implies

$$\left.\begin{aligned}X_D(w,\sigma)&=-\frac{1+\sigma^2}{3(1-\sigma^2)^2}-\frac{w^2(1+14\sigma^2+\sigma^4)}{15(1-\sigma^2)^4}-\\&\frac{w^4(3+125\sigma^2+125\sigma^4+3\sigma^6)}{105(1-\sigma^2)^6}+\ldots\\X_K(w,\sigma)&=\frac{2}{3(1-\sigma^2)^2}+\frac{8w^2(1+\sigma^2)}{15(1-\sigma^2)^4}+\\&\frac{w^4(54+148\sigma^2+54\sigma^4)}{105(1-\sigma^2)^6}+\ldots\end{aligned}\right\}, \quad \textbf{(96)}$$

and

$$M(w,\sigma)=\frac{4}{\pi}[X_D(w,\sigma)D(\sigma)+X_K(w,\sigma)K(\sigma)]. \quad \textbf{(97)}$$

The limiting case gives

$$\frac{\Phi_{\mathrm{L}}}{\Phi_0}\approx 1-\frac{2}{\pi v_0}\cdot[4D(\sigma)/\pi+w_0^2 M(w_0,\sigma)]. \quad \textbf{(98)}$$

In the Fraunhofer case, one has $w_0=0$, and only the first term in the square brackets contributes. The non-limiting case gives

$$\frac{\Phi_{\mathrm{NL}}}{\Phi_0}\approx 1+\frac{2}{\pi v_0}\cdot[(1-\sigma^2)^2 M(\omega,\sigma)]. \quad \textbf{(99)}$$

7. TREATMENT OF MULTIPLE WAVELENGTHS

Quantities v_0, u and $v_\pm$ are all proportional to λ^{-1}. Diffraction effects on spectral power at small λ can be described using

$$\frac{\Phi_\lambda(\lambda)}{\Phi_\lambda^0(\lambda)}\approx 1-\lambda a_0'(\lambda)-\lambda^{7/2}\{a_B'(\lambda)+[a_B'(\lambda)]^*\} \quad \textbf{(100)}$$

for limiting geometries, or using

$$\frac{\Phi_\lambda(\lambda)}{\Phi_\lambda^0(\lambda)}\approx 1+\lambda a_0(\lambda)+\lambda^{7/2}\{a_B(\lambda)+[a_B(\lambda)]^*\}+ \lambda^3\{a_X(\lambda)+[a_X(\lambda)]^*\} \quad \textbf{(101)}$$

for non-limiting geometries. Here, $\Phi_\lambda(\lambda)$ and $\Phi_\lambda^0(\lambda)$ are the spectral power that reaches the detector with and without diffraction. Several of the a functions above involve other smooth "envelope" functions of λ times complex exponentials:

$$a_B(\lambda)=b_-(\lambda)e^{2iv_-}+b_+(\lambda)e^{2iv_+}, \quad \textbf{(102)}$$

$$a_B'(\lambda)=b_-'(\lambda)e^{2iv_-}+b_+'(\lambda)e^{2iv_+} \quad \textbf{(103)}$$

$$\begin{aligned} a_X(\lambda)=\ & c_{1,-}(\lambda)e^{-i\varphi_1(v_-)}+c_{1,+}(\lambda)e^{-i\varphi_1(v_+)}+ \\ & c_{2,-}(\lambda)e^{-i\varphi_2(v_-)}+c_{2,+}(\lambda)e^{-i\varphi_2(v_+)}. \end{aligned} \quad \textbf{(104)}$$

This can be reasonably expected because of the asymptotic properties of diffraction effects derived in earlier sections.

The envelope functions behave like power series' at small λ. There, they can be found using interpolation once they have been evaluated at a few values of λ. Rearranging the phase factors and a leading power of λ into multipliers of the envelope functions as shown in Eq. (100-104) facilitates this. If one can establish a λ_m, so that the above decomposition is established as adequate for all $\lambda<\lambda_m$, Gauss-Chebyshev quadrature according to sampling at regularly spaced values of θ with $\lambda=\lambda_m(1+\cos\theta)/2$ similar to that presented in Section 6 can expedite treatment of a very large number of short wavelengths.

To derive the envelope functions for the main diffraction effects, we note that, from Eq. (1-3) and Eq. (70), one can deduce

$$a_0'(\lambda)=\frac{1}{\pi\lambda}\int_{-1}^{+1}dx\, G(\sigma,x)L_{\mathrm{n.o.}}(v,w) \quad \textbf{(105)}$$

and

$$b_\pm'(\lambda)=\mp\frac{1}{\pi\lambda^{7/2}}\left(\frac{i}{v_0\sigma}\right)\int_0^\infty dt\, e^{-t^2}tG(\sigma,x)L_+(v,w), \quad \textbf{(106)}$$

with $x=\pm 1+it^2/(2v_0\sigma)$, $v=v_0(1+\sigma x)$ and $w=u/v$ in the limiting case, as well as

$$a_0(\lambda)=\frac{1}{\pi\lambda}\left(\frac{u}{v_0}\right)^2\int_{-1}^{+1}dx\, G(\sigma,x)w^2L_{\mathrm{n.o.}}(v,w). \quad \textbf{(107)}$$

and

$$b_\pm(\lambda)=\mp\frac{1}{\pi\lambda^{7/2}}\left(\frac{u}{v_0}\right)^2\left(\frac{i}{v_0\sigma}\right)\int_0^\infty dt\, e^{-t^2}tG(\sigma,x)w^2L_+(v,w), \quad \textbf{(108)}$$

with $w=v/u$ in the non-limiting case. To derive the envelope functions for the remaining effects, one can implement the change of variables as outlined for Eq. (80-81). This gives

$$c_{\mu,\pm}(\lambda)=\pm\frac{1}{\pi\lambda^3}\left(\frac{u}{v_0}\right)^2\int_0^\infty dt\left(\frac{dv}{dt}\right)e^{-t^2}M(v,v_0)Q_\mu(u,v) \quad \textbf{(109)}$$

with the dependence of v on t defined by the contour with the same subscripts as the envelope function in Eq. (81). Gauss-Chebyshev and Gauss-Hermite quadrature facilitate all integrations in Eqs. (105-109).

8. RADIOMETRIC APPLICATION EXAMPLES

Radiometric applications that feature small diffraction corrections include total solar irradiance measurements. A variety of instrument designs exist, many of which are discussed in Ref. [19] and Ref. [20], which amends geometrical layouts reported in Ref. [19]. Two examples are the PMO6 that is described by Brusa and Fröhlich [21] and the Total-Irradiance Monitor (TIM) that is described by Lawrence *et al.*[22]. Both designs involve an electrical-substitution radiometer (ESR) sensing total optical power incident on a cavity entrance. In an ESR, measurement accuracy is achieved by equating the difference in electric power delivered by resistive heating to the cavity required to maintain a constant temperature when a shutter is closed versus open to the optical power delivered when the shutter is open. In this way, the accuracy achievable for electrical power measurements is transferred as much as is feasible to the optical power measurements.

Table 1. Parameters and diffraction effects for sample SAD systems

Parameter	Optical System: PMO6	TIM	Blackbody
R_s (mm)	6.75×10^{11}	6.75×10^{11}	58.78195
R_a (mm)	4.25	3.9894	0.050
R_d (mm)	2.5	7.62	9.99871
d_s (mm)	1.5×10^{14}	1.5×10^{14}	160.0718
d_d (mm)	95.4	101.6	914.679
Φ/Φ_0, $T=5900$ K	1.0012716882	0.9995771968	
$\Phi_\lambda/\Phi_{0,\lambda}$, $\lambda=\lambda_e(5900\text{ K})$	1.0012707926	0.9995771897	

PMO6 has a non-limiting aperture that is upstream from the cavity entrance that reduces stray light but results in excess power as reported in Ref. [21], whereas TIM has a limiting aperture upstream from the cavity that defines the total power but also leads to a diffraction-induced loss in flux [22]. Laboratory-based characterization of these and other instruments can involve laser-based monochromatic studies such as those conducted in Ref. [23] and Ref. [24]. In such instances diffraction effects on spectral power are also pertinent. For these instruments, we have re-evaluated previous diffraction effects on total power and spectral power at the effective wavelength for a 5900 K blackbody and tabulate results in Table 1. Diffraction effects on total power and its effective-wavelength spectral-power proxy are both included for the solar instruments. The blackbody has a variable temperature, whereas the sun's surface temperature was assumed to be 5900 K. The digits shown in the ratios are significant if one wants to check numerical methods. Uncertainties of input parameters would also contribute to the uncertainty of results. The effective wavelength is $\lambda_e = \zeta(3)c_2/(3\zeta(4)T)$. With it, the A_{-1} term in Eq. (39) in the spectral case and the C_{-3} term in Eq. (9) in the thermal case give rise to the same relative diffraction effect, as emphasized, for instance, by Blevin.[7] The result for total power for PMO6 differs by about 0.000008 from our previous result due to a correction in the treatment of extended-source effects. Regarding the spectral power, the present result relies on the extended-source methodology described in Section 6. The efficacy of the interpolation procedure described in Section 7 is illustrated in Fig. 2, where all oscillatory contributions and their sum are shown. These results are based on calculations with the efficient contour integrals at 8 wavelengths over the range $\lambda = 0$ mm to $\lambda = 0.00825$ mm, with an accuracy of 10^{-8} of the total flux.

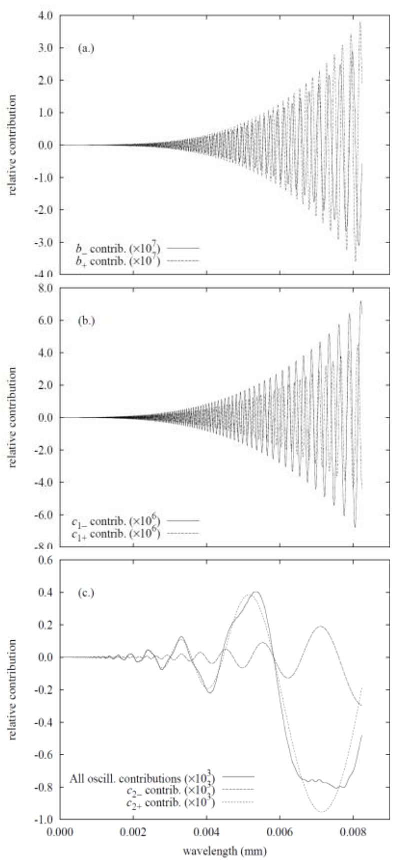

Fig. 2. Shown are b_- and b_+ oscillatory contributions vs. wavelength for PMO6 (a), c_{1-} and c_{1+} contributions (b), and c_{2-} and c_{2+} contributions (c). All are scaled for presentation. The sum of all oscillatory contributions is also presented in panel (c).

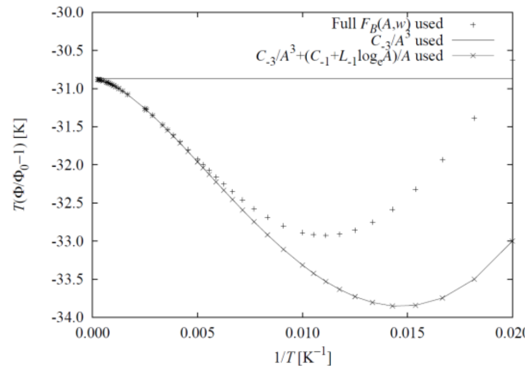

Fig. 3. Relative diffraction loss multiplied by temperature for several temperatures larger than 50 K (points), and approximated using the leading term (line) and using the leading three terms (lines with points).

Significant diffraction corrections are typified by losses incurred when a cryogenic blackbody is viewed through a pinhole aperture by an active-cavity radiometer. For upcoming tests in the NIST Low-Background Infrared Radiometry (LBIR) facility [25], anticipated geometrical parameters are also indicated in Table 1. Not shown are non-limiting baffles between the pinhole and radiometer, which should have a much smaller effect but could also merit attention. In Fig. 3, we indicate diffraction effects on total power over a temperature range that brackets upcoming measurements. Contributions of first-order and next-leading-order approximations are also indicated. The temperature-scaled first-order effect is a constant, and the next terms vary as combinations of $1/T^2$ and $[\log_e(\alpha T/c_2)]/T^2$. This illustrates the limitations of order-by-order asymptotic expansions for diffraction effects as well as the efficacy of Eq. (68) to include the remainder term. Reference [26] also provides an example with significant diffraction effects that are also strongly affected by having a finite size of source. This reference also demonstrates that large diffraction losses can arise in for far-infrared measurements.

Several benefits of the work can be deduced from the above examples. It is anticipated that these benefits will be helpful to many, the author included. First, integration of diffraction-corrected spectral power over the entire Planck spectrum to obtain the diffraction-corrected total power is obviated. Second, the treatment of extended sources is possible without the need to perform integrals of oscillatory functions, which was not the case in Ref. [17]. Third, the calculation of diffraction effects for a large number of wavelengths is now possible with a very low computational cost. One area of radiometry that can benefit from this is the calibration of filter radiometers, such as can be done using the methods of Ref. [23]. In that case, power-stabilized, wavelength-stabilized laser light can be fiber-fed into an integrating sphere to obtain an extended quasi-monochromatic, quasi-Lambertian source. (This typically requires submerging a portion of the fiber in a vibrating water bath to minimize speckle. The complex form of the actual in-band and out-of-band transmittance of a filter can necessitate detailed wavelength sampling, and the diffraction effects for such a large number of wavelengths is clearly in-hand thanks to the methods detailed in Section 7.

9. CLOSING REMARKS

The methods presented here for evaluating diffraction effects each have ranges of validity. For large A or small v, direct numerical methods to evaluate the effects are possible and numerically expedient. At small A or large v, leading terms in the asymptotic expansions of $F_B(A,w)$,

$F_X(A,w)$, $L_B(\nu,w)$ and $L_X(\nu,w)$ can be sufficiently accurate. Otherwise, methods presented here can be used to evaluate these functions. For extended sources, integration of oscillatory terms in $L_B(\nu,w)$ and $L_X(\nu,w)$ can be done numerically as in Eq. (3) when these functions oscillate slowly, or according to the methods with deformed contours in cases of rapid oscillations. Likewise, repeated calculations for a large of number of wavelengths can be avoided in spectral regions that feature large ν by interpolation methods. Hence, except for rare cases emphasizing edge effects in the sense of allowing one to have w too close to unity, an accurate result that is analytically compact and/or numerically tractable can be found for single-edge diffraction effects in a wide variety of symmetric systems.

One caveat also deserves mention. The concept of an incoherent Lambertian source is itself an unrealistic idealization as was noted by Walther [27, 28]. Carter and Wolf [29] discuss coherence properties of Lambertian and non-Lambertian sources, and Wolf [30] summarizes the interplay and tension between coherence that always exists for real light fields and classical radiometry, the latter being a topic, of which this work only addresses a subtopic, viz. diffraction corrections. A survey of the studies of diffraction effects that are cited in the present work shows that the quantitative validity of this work is still defensible in practical radiometry. In this regard, there is one very recent example [31] in which a laser was fiber-fed into an integrating sphere source that was presented to a trap detector through an intermediate aperture. There, a treatment of diffraction consistent with this work was shown to account well for diffraction effects, even while neglecting coherence issues. However, the issues raised beginning with Walther's analysis are a topic of interest of which one should always be mindful, especially in cases of novel types of measurement.

Acknowledgment. I thank T.A. Germer, T. Wong and Z.H. Levine for helpful comments.

APPENDIX

Consider a Planck source at temperature $T = c_2/(2\pi\beta)$, where c_2 is the second radiation constant. Hence, this also defines β. Suppose radiation is emitted at a point on the source and can follow various paths to arrive at a point on a detector. For purposes of knowing the related contribution to the total irradiance at the latter point, the function

$$\begin{aligned} S(\beta,l) &= \textstyle\sum_{n=1}^{\infty}[(l-in\beta)^{-4}+(l+in\beta)^{-4}] \\ &= 2\zeta(4)/\beta^4 - 20\zeta(6)l^2/\beta^6 + \ldots \end{aligned} \qquad \textbf{(A1)}$$

helps quantify interference of two contributions to the field that traveled over paths with relative path length difference l. Summation over n leads to the zeta function of Riemann. If we set $z = 2\pi l/\beta$ and $f = 1/(1-e^{-z})$, we can rewrite this as

$$S(\beta,l) = -\left(\frac{2\pi}{\beta}\right)^4 [z^{-4} + (f - 7f^2 + 12f^3 - 6f^4)/6]. \qquad \textbf{(A2)}$$

At small z, this becomes

$$S(\beta,l) = 32\pi^4/\beta^4(1/1440 - z^2/6048 + z^4/69120 - \ldots). \qquad \textbf{(A3)}$$

Mellin transforms

$$\Sigma(\beta,\nu) = \textstyle\int_0^{\infty} dl\, l^{\nu} S(\beta,l) \qquad \textbf{(A4)}$$

and

$$\Sigma_L(\beta,\nu) = \textstyle\int_0^{\infty} dl\, l^{\nu} S(\beta,l)\log_e l \qquad \textbf{(A5)}$$

are bounded for $-1 < \Re\nu < 3$. One way to evaluate the first case involves replacing integration along the positive real axis with integration along two contours:

$$\int_0^{\infty} dl\, l^{\nu} S(\beta,l) = \frac{1}{2}\textstyle\int_{C_+} dl\, l^{\nu} S(\beta,l) + \frac{1}{2}\int_{C_-} dl\, l^{\nu} S(\beta,l). \qquad \textbf{(A6)}$$

Obviously, each contour could run from zero to $+\infty$. We place the branch cuts of $\log_e l$ and l^{ν} (the latter required for non-integer ν) on the negative real axis with $l^{\nu} > 0$ and $\log_e l$ being real for $l > 0$. For each term in $S(\beta,l)$ having a pole on the positive imaginary axis, we instead deform C_+ to begin at zero, run just above the negative real axis to $-\infty$ and along an infinitely large semicircular arc in the upper half plane to $+\infty$. However, the contour must also take an excursion from the arc to enclose the pole in a positive sense. For each term in the sum with no such pole, no excursion is required. We modify C_- correspondingly in the lower half plane. Contributions to $\Sigma(\beta,\nu)$ from along the negative real axis are

$$\frac{1}{2}\left[-e^{i\pi\nu}\Sigma(\beta,\nu) - e^{-i\pi\nu}\Sigma(\beta,\nu)\right] = -\cos(\pi\nu)\Sigma(\beta,\nu), \qquad \textbf{(A7)}$$

contributions from arcs are zero, and contributions from poles are

$$\begin{aligned} &\frac{i\pi\nu(\nu-1)(\nu-2)\zeta(3-\nu)}{6\beta^{3-\nu}}(e^{i\pi(\nu-3)/2} - e^{-i\pi(\nu-3)/2}) = \\ &-\frac{\pi\nu(\nu-1)(\nu-2)\zeta(3-\nu)}{3\beta^{3-\nu}}\sin\left(\frac{\pi(\nu-3)}{2}\right). \end{aligned} \qquad \textbf{(A8)}$$

The latter involve third derivatives of l^{ν} at $l = e^{\pm i\pi/2}n\beta$. Equating the combination of the above two expressions with $\Sigma(\beta,\nu)$ gives

$$\Sigma(\beta,\nu) = -\frac{\pi\nu(\nu-1)(\nu-2)\zeta(3-\nu)}{3\beta^{3-\nu}[1+\cos(\nu\pi)]}\sin\left[\frac{\pi(\nu-3)}{2}\right]. \qquad \textbf{(A9)}$$

Evaluating this for ν approaching 0, 1 or 2, we have $\Sigma(\beta,0) = 0$, $\Sigma(\beta,1) = -\zeta(2)/(3\beta^2)$, and $\Sigma(\beta,2) = -\pi/(3\beta)$. The $\nu = 2$ result relies on $\zeta(1+\varepsilon) = 1/\varepsilon + \gamma + O(\varepsilon)$. Using

$$\begin{aligned} &\frac{\Sigma_L(\beta,\nu)}{\Sigma(\beta,\nu)} = \frac{d}{d\nu}\log_e \Sigma(\beta,\nu) = \frac{1}{\nu} + \frac{1}{\nu-1} + \frac{1}{\nu-2} - \\ &\frac{\zeta'(3-\nu)}{\zeta(3-\nu)} + \frac{\pi}{2}\cot\left[\frac{\pi}{2}(\nu-3)\right] + \log_e\beta + \frac{\pi\sin(\pi\nu)}{1+\cos(\pi\nu)} \end{aligned} \qquad \textbf{(A10)}$$

and $\zeta'(1+\varepsilon) = -1/\varepsilon^2 + O(1)$ gives $\Sigma_L(\beta,0) = -\pi\zeta(3)/(3\beta^3)$, $\Sigma_L(\beta,1) = -[\zeta(2)\log_e\beta - \zeta'(2)]/(3\beta^2)$ and $\Sigma_L(\beta,2) = \pi(2\gamma - 3 - 2\log_e\beta)/(6\beta)$.

Transforms

$$\Xi(\beta,\nu) = \textstyle\int_0^{\infty} dl\, l^{\nu}[S(\beta,l) + l^{-4}] \qquad \textbf{(A11)}$$

and

$$\Xi_L(\beta,\nu) = \textstyle\int_0^{\infty} dl\, l^{\nu}\{[S(\beta,l) + l^{-4}]\log_e l\} \qquad \textbf{(A12)}$$

are bounded for $\Re\nu < 3$. Rearranging $S(\beta,l)$ gives

$$S(\beta,l) + \frac{1}{l^4} = \frac{(2\pi)^4}{6\beta^4}\sum_{n=1}^{\infty} n^3 e^{-nz} \qquad \textbf{(A13)}$$

and

$$\Xi(\beta,\nu) = \frac{(2\pi)^4}{6\beta^4}\sum_{n=1}^{\infty} n^3 \int_0^{\infty} dl\, l^{\nu} e^{-nz}$$
$$= \frac{1}{6}\left(\frac{2\pi}{\beta}\right)^{3-\nu} \Gamma(\nu+1)\zeta(\nu-2) = 2^{\nu+1}\beta^{\nu-3}\chi(\nu), \quad \textbf{(A14)}$$

with $\chi(\nu) = \Gamma(\nu+1)\zeta(\nu-2)/[96(4\pi)^{\nu-3}]$, and

$$\Xi_L(\beta,\nu) = \frac{d}{d\nu}\Xi(\beta,\nu)$$
$$= 2^{\nu+1}\beta^{\nu-3}[\xi(\nu) + \log_e \beta]\chi(\nu), \quad \textbf{(A15)}$$

with $\xi(\nu) = \psi(\nu+1) + \zeta'(\nu-2)/\zeta(\nu-2) - \log_e(2\pi)$.

References

1. L. Rayleigh, "On Images formed without Reflection or Refraction," Phil. Mag. **11**, 214-218 (1881).
2. E. Lommel, "Die Beugungserscheinungen einer kreisrunden Oeffnung und eines kreisrunden Schirmschens theoretisch und experimentell Bearbeitet," Abh. Bayer. Akad. **15**, 233-328 (1885).
3. J. Focke, "Total illumination in an aberration-free diffraction image," Optica Acta **3**, 161-163 (1956).
4. E. Wolf, "Light Distribution Near Focus in an Error-Free Diffraction Image," Proceedings of the Royal Society A: Mathematical, Physical and Engineering Sciences **204**, 533-548 (1951).
5. C. L. Sanders and O. C. Jones, "Problem of Realizing the Primary Standard of Light," Journal of the Optical Society of America **52**, 731-742 (1962).
6. N. Ooba, "Experimental Study on Diffraction in the Measurement of the Primary Standard of Light," Journal of the Optical Society of America **54**, 357-361 (1964).
7. W. R. Blevin, "Diffraction Losses in Radiometry and Photometry," Metrologia **6**, 39-44 (1970).
8. W. H. Steel, M. De, and J. A. Bell, "Diffraction Corrections in Radiometry," Journal of the Optical Society of America **62**, 1099-1103 (1972).
9. L. P. Boivin, "Diffraction corrections in radiometry: comparison of two different methods of calculation," Appl Opt **14**, 2002-2009 (1975).
10. E. L. Shirley, "Revised formulas for diffraction effects with point and extended sources," Applied Optics **37**, 6581-6590 (1998).
11. P. Edwards and M. McCall, "Diffraction loss in radiometry," Applied Optics **42**, 5024-5032 (2003).
12. K. D. Mielenz, "Spectroscope Slit Images in Partially Coherent Light," Journal of the Optical Society of America **57**, 66-74 (1967).
13. C. E. Dionne, "Spectral resolution modeling with partial coherence for the Atmospheric Infrared Sounder instrument," Optical Engineering **47**, 026402-026401 to 026402-026407 (2008).
14. E. L. Shirley and M. L. Terraciano, "Two innovations in diffraction calculations for cylindrically symmetrical systems," Applied Optics **40**, 4463-4472 (2001).
15. E. L. Shirley, "Intuitive diffraction model for multistaged optical systems," Applied Optics **43**, 735-743 (2004).
16. E. L. Shirley, "Higher-order boundary-diffraction-wave formulation," Journal of Modern Optics **54**, 515-527 (2007).
17. E. L. Shirley, "Diffraction corrections in radiometry: spectral and total power and asymptotic properties," Journal of the Optical Society of America A **21**, 1895-1906 (2004).
18. C. Lanczos, *Tables of Chebyshev Polynomials S_n(x) and C_n(x)*, National Bureau of Standards Applied Mathematics Series (G.P.O., Washington, D.C., 1952), Vol. 9.
19. J. J. Butler, B. C. Johnson, J. P. Rice, E. L. Shirley, and R. A. Barnes, "Sources of Differences in On-Orbital Total Solar Irradiance Measurements and Description of a Proposed Laboratory Intercomparison," Journal of Research of the National Institute of Standards and Technology **113**, 187-203 (2008).
20. B. C. Johnson, M. Litorja, J. B. Fowler, E. L. Shirley, R. A. Barnes, and J. J. Butler, "Results of aperture area comparisons for exo-atmospheric total solar irradiance measurements," Applied Optics **52**, 7963-7980 (2013).
21. R. W. Brusa and C. Fröhlich, "Absolute radiometers (PMO6) and their experimental characterization," Applied Optics **25**, 4173-4180 (1986).
22. G. M. Lawrence, G. Kopp, G. Rottman, J. Harder, T. Woods, and H. Loui, "Calibration of the total irradiance monitor," Metrologia **40**, S78-S80 (2003).
23. S. W. Brown, G. P. Eppeldauer, and K. R. Lykke, "Facility for spectral irradiance and radiance responsivity calibrations using uniform sources," Applied Optics **45**, 8218-8237 (2006).
24. G. Kopp, K. Heuerman, D. Harber, and G. Drake, "The TSI Radiometer Facility: absolute calibrations for total solar irradiance instruments," Proc. of SPIE **6677**, 667709-667701-667712 (2007).
25. A. C. Carter, T. M. Jung, A. Smith, R. L. Steven, and R. Datla, "Improved broadband blackbody calibrations at NIST for low-background infrared applications," Metrologia **40**, S1-S4 (2003).
26. F. C. Witteborn, M. Cohen, J. D. Bregman, D. H. Wooden, K. Heere, and E. L. Shirley, "Spectral Irradiance Calibration in the Infrared. XI. Comparison of α Bootis and 1 Ceres with a Laboratory Standard," The Astronomical Journal **117**, 2552-2560 (1999).
27. A. Walther, "Radiometry and Coherence," Journal of the Optical Society of America **58**, 1256-1259 (1968).
28. A. Walther, "Radiometry and coherence," Journal of the Optical Society of America **63**, 1622-1623 (1973).
29. W. H. Carter and E. Wolf, "Coherence properties of lambertian and non-lambertian sources," Journal of the Optical Society of America **65**, 1067-1071 (1975).
30. E. Wolf, "Coherence and radiometry," Journal of the Optical Society of America **68**, 6-17 (1978).
31. S. G. R. Salim, S. Briaudeau, F. Bourson, B. Rougié, D. Truong, O. Kozlova, J. M. Coutin, and M. Sadli, "A reference radiance-meter system for thermodynamic temperature measurements," Metrologia **53**, 945-955 (2016).